Early forest fire detection by vision-enabled wireless sensor networks

Suggested running head: Early fire detection by vision-enabled WSNs

Jorge Fernández-Berni[A,C], *Ricardo Carmona-Galán*[A], *Juan F. Martínez-Carmona*[B], *Ángel Rodríguez-Vázquez*[A]

[A] Institute of Microelectronics of Seville (IMSE CNM-CSIC-US), Avda. Américo Vespucio s/n, Seville (Spain)

[B] Andalusian Forest Fire Suppression and Prevention Service (INFOCA), Avda. Manuel Siurot 50, Seville (Spain)

[C] Corresponding author. Email: berni@imse-cnm.csic.es

Abstract: Wireless sensor networks constitute a powerful technology especially suitable for environmental monitoring. With regard to wildfires, in particular, they enable low-cost fine-grained surveillance of hazardous locations like wildland urban interfaces. This paper presents the work developed during the last four years targeting a vision-enabled wireless sensor network node for the reliable, early on-site detection of forest fires. The tasks carried out ranged from devising a robust vision algorithm for smoke detection to the design and physical implementation of a power-efficient smart imager tailored to the characteristics of such an algorithm. By integrating this smart imager with a commercial wireless platform, we endowed the resulting system with vision capabilities and radio communication. Numerous tests were arranged in different natural scenarios in order progressively to tune all the parameters involved in the autonomous operation of this prototype node. The latest test carried out, involving the prescribed burning of a 95m×20m shrub plot, has confirmed the high degree of reliability of our approach in terms of both successful early detection and very low false alarm rate.

Brief summary: This paper presents a vision-enabled wireless sensor network node for early detection of forest fires. By integrating a prototype smart imager with a commercial wireless platform, we endowed the resulting system with vision capabilities and radio communication. The tests arranged have confirmed the high degree of reliability of our approach.

Additional keywords: smoke detection, false alarm rate, energy efficiency, artificial vision, focal-plane processing, VLSI implementation

Introduction

A Wireless Sensor Network, WSN (Pottie 2000; Akyildiz *et al.* 2002), can be defined as a set of low-power low-cost nodes with different sensing capabilities deployed throughout a region of interest. Processing and radio communication are also enabled on each sensor node. Due to these characteristics, WSNs are suitable for implementing environmental monitoring systems supported by fine-grained spatio-temporal sensing grids. With regard to forest fires, the WSN-based monitoring systems reported to date have been intended to predict rather than detect forest fires (Kremens *et al.* 2003; Chaczko and Amad 2005; Doolin and Sitar 2005; Son *et al*. 2006; Hefeeda 2007; Machado *et al.* 2010). This is because the available sensing modules have, in most cases, been restricted to scalar measurements like relative humidity, temperature or wind speed. These systems can therefore only determine the probability and eventual intensity of fire ignition from the observations of the environmental conditions provided by the sensors. Obviously, the nodes could still detect increases in temperature and decreases in barometric pressure and humidity from flame fronts before they burn, but very dense deployment is needed in order to detect a fire before it spreads (Fierens 2009).

A new possibility concerning WSN sensing capabilities has recently begun to be explored: that of multimedia sensing (Eren and Akan 2005; Akyildiz *et al.* 2007). In our case, the incorporation of artificial vision – meaning image sensing plus analog and digital processing plus video analytics and the obtaining of the targeted result – is of great interest. It would make it possible not only to monitor a certain area from the perspective of environmental conditions,

but also to carry out visual inspection for the early detection of smoke or flames. However, the implementation of vision hardware in WSN nodes is not at all a trivial matter. The visual stimulus involves handling a massive flow of multidimensional information. Taking into account the very strict power budget allocated to each node, the capture and digitization of one image sequence alone could represent a significant percentage of its energy consumption. But the critical point arises just afterwards. On one hand, the sequence could be simply transmitted for remote processing, dramatically affecting the scalability and bandwidth of the network. On the other hand, the node itself could deal with the image sequence using its own processing capabilities. In this case, the nature of such processing is greatly influenced by energy constraints, and new strategies are therefore required which would allow early visual detection with the minimum possible power consumption. It is precisely on this need for new strategies to enable local image processing in WSN nodes that this paper focuses.

Objectives

Early detection and accurate location are two crucial points when it comes to preventing forest fires from spreading. The intervention of fire suppression resources becomes much more efficient if an alarm signal containing the geographical coordinates of the fire is delivered within a time interval of 15 minutes (INSA 2000). Ground systems (Sistema Bosque 1999; Kuhrt *et al.* 2001; Fire Watch 2004; Stipanicev *et al.* 2010) are currently the only systems capable of detecting a fire within a few minutes of its outbreak. They rely on cameras monitoring large areas. This means that a small number of cameras suffice to survey an extensive region. But it also means that detection is quite difficult as smoke can appear at very distant locations, triggering numerous false alarms (Arrue *et al.* 2000; Schroeder 2004) and requiring cameras featuring huge pixel resolution (Fernández-Berni *et al.* 2008). Moreover, these systems are quite expensive (Schroeder 2005). If infrared technology is to be used, costly calibration cycles push budgets up considerably. On the other hand, current WSN-based systems rely, as previously mentioned, on low-cost sensors which only monitor the environmental conditions around them. Very dense sensor deployment is therefore crucial to early detection. We propose to merge these

two approaches together to achieve robust, scalable and reliable detection of forest fires with appropriate temporal and spatial resolution. The resulting system would be based on the sparse deployment of smart vision-enabled sensors constituting a wireless network. These sensors would on-site run a vision algorithm tailored to detect smoke arising from areas of vegetation which are small in comparison with the areas surveyed by cameras in ground systems. When a sensor detects smoke, a warning message is sent to a control center by multi-hopping through the network. A sketch of the system is shown in Fig.1, where A_{S_i} represents the area surveyed by the sensor S_i. This system offers several advantages when compared to current automatic ground systems, namely:

- **Robustness**: The failure of one sensor affects only a very small fraction of the surveyed region.
- **Scalability**: Monitoring small areas, the layout of the sensor network can be adapted to the particular characteristics of the region to be surveyed.
- **Reliability**: The vision sensors analyze not landscape images but small areas of vegetation. Detection is therefore made easier and typical sources of false alarms like clouds or smoke rising from factories are avoided.
- **Better temporal resolution**: Thanks also to the small size of the areas surveyed by the sensors, smoke can be detected within short time intervals, typically a few minutes at most.
- **Simpler smoke location**: Complex GIS software is necessary for smoke location in commercial ground systems. In a system based on smart vision sensors, each sensor could store the geographic reference of the area it is surveying and include it in the alarm message. This would suffice easily to locate the fire.

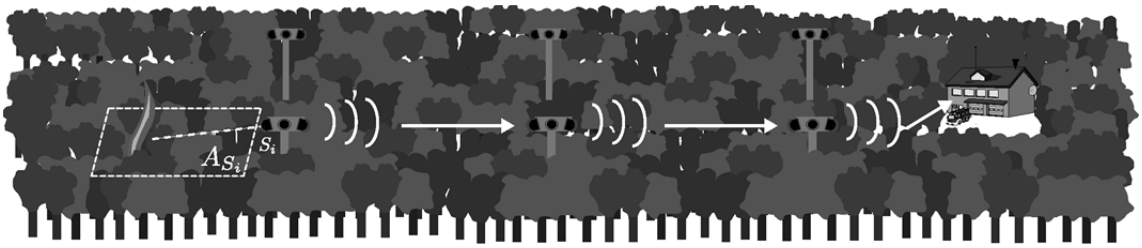

Fig. 1: Sketch of the proposed system.

With respect to the WSN-based systems reported so far in literature, the incorporation of vision makes dense deployments for early detection unnecessary. The sensors do not now have to be very close to the fire to detect its presence. This implies a significant reduction in the number of sensor nodes, and this in itself a significant step forward in terms of the cost and maintenance of the system as a whole.

Naturally, the benefits of the proposed system do not come totally free of charge. They essentially depend on the successful fulfilment of this work's primary objective; i.e. the efficient integration of vision capabilities into the sensing nodes. Bear in mind that we want the sensors constantly to run a vision algorithm at the minimum possible energy cost in order to prolong the life of their batteries as much as possible.

Methodology

A vision algorithm for smoke detection

A crucial element in our approach is a reliable vision algorithm for smoke detection in the scenario just described. Numerous vision algorithms for forest fire smoke detection have been reported in literature (de Vries and Kemp 1994; den Breejen *et al.* 1998; Vicente and Guillemant 2002; Gómez-Rodríguez *et al.* 2002; Toreyin *et al.* 2007; Krstinic *et al.* 2009). All of them analyze images coming from remote cameras surveying large areas. They have to deal with cloud motion, dust etc. in order to reduce the false alarm rate. In the system above proposed, however, the sensors watch small areas and most of the pixels of the images that are processed will therefore correspond to nearby vegetation. This means that the potential sources

of false alarms are totally different. The movement which now has to be filtered is that of tree leaves, birds or even people walking around. We would also like to point out that, from a more general point of view, smoke detection can be seen as a case study in dynamic texture recognition (Fernández-Berni *et al.* 2009).

As a preliminary step, the image plane is divided into regular regions with a size of W×H pixels. The processing is then focused only on the mean value of the pixels corresponding to each region. Despite its simplicity, we will demonstrate that such reduced scene representation suffices for reliable smoke detection. Moreover, this objective can be achieved very efficiently by using one of the processing primitives implemented by our smart imager, as described later. In terms of image processing, the main effect caused by smoke rising against a vegetation background is the increased luminance in the regions affected. Indeed, if RGB images are being processed, the effect would be not only the increase of each component but also their equalization (Chen *et al.* 2006). Going one step further, we have found that the most sensitive component to the presence of smoke in such conditions is the blue component (Fernández-Berni *et al.* 2008). As an example, consider Fig. 2. We have marked a zone within a scene in which the background mainly comprises vegetation. The intensity histogram of the RGB components and the luminance is then represented under two situations: without smoke and with the presence of smoke. It can be seen that, without smoke, most of the pixels of the B component present the lowest intensity values. When smoke appears, the RGB components and the luminance increase and equalize their intensities. Note that the vertical axis of the histograms represents the number of pixels of the corresponding component featuring the intensity value indicated by the horizontal axis, within a scale of 256 values.

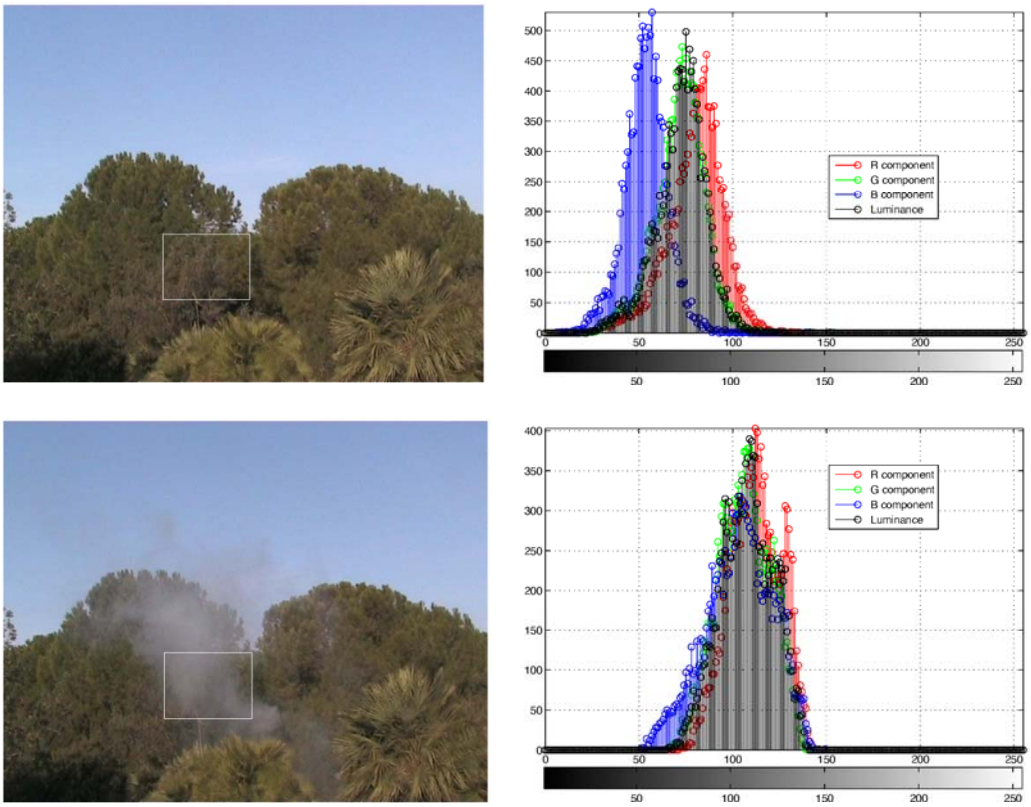

Fig. 2: Intensity histogram of the RGB components and luminance of a vegetation zone without smoke and with the presence of smoke.

To establish a numerical reference, we have calculated the normalized average increase, with reference to the background, undergone by each component of the pixels within the marked zones when smoke appears. The results are summarized in Table 1. We can see that the appearance of smoke among vegetation means a greater increase for the B component than for the R and G components and the luminance. The B component is therefore the most sensitive to the presence of smoke. These results are coherent with the reflectance spectra of typical fresh and dry vegetation (Jacquemoud *et al.* 1994).

Table 1. Normalized average increase, with reference to the background, undergone by each component of the pixels within the zones marked in Fig. 2 when smoke appears.

	R component	G component	B component	Luminance
Increase	12.5%	13.4%	19.5%	13.8%

All in all, the first stage of the algorithm has to do with a possible increase detected at any of the W×H regions in the image plane division. A region (k, l) will be considered a candidate to contain smoke when its foreground intensity I_{kl_F} fulfills the following equation:

$$I_{kl_F} \geq I_{kl_B} + q \tag{1}$$

where I_{kl_B} is the background intensity of that same region (k, l) and q is a parameter indicating the minimum increase in intensity a region must undergo if it is to be considered a candidate to contain smoke. We are assuming that foreground images are captured at a fixed time interval denoted as T_F. Note that Eq. (1) requires the existence of a background model. In our first approach to this model (Fernández-Berni *et al.* 2010) we considered that, since the background of the scenes inspected by the algorithm is mostly composed of vegetation, it rarely undergoes significant changes. As long as no candidate region had been detected from the previous frame, the background was therefore simply represented by sporadically updated frames. However, in the different field tests we carried out, we noticed that this very simple model, while working well under most operational conditions, was not adequate for vegetation areas affected by sudden changes in illumination; for example, when the sun is partially occluded by fast moving clouds. In such a case, a significant number of false candidate regions can be triggered, masking the presence of true candidate regions containing smoke. To deal with this, we modified the background model. Now, whenever certain spatio-temporal dynamics of candidate regions are dismissed, the background is updated with the next frame. Those changes which could prevent smoke from being adequately segmented and analyzed by the algorithm are therefore constantly being incorporated into the background representation. This modification has proven to endow the algorithm with very high reliability and robustness.

The second stage of the algorithm, once candidate regions have been detected, consists of searching for spatio-temporal patterns characteristic of smoke dynamics. This stage is divided into two phases: a detection phase and a confirmation phase. The detection phase starts when the first candidate regions are discovered, an instant denoted as t_0, and finishes at $t = t_D$. The confirmation phase is then initiated. This phase will last T_C seconds at most if smoke is really

present, finishing at time $t = t_C$ by sending an alarm message. The internal processing in both phases works as follows. First of all, in order to consider that smoke is present at the scene, a minimum number of candidate regions must exist. Let us define $N(t)$ as the number of candidate regions at time instant t. This parameter can change every T_F seconds - that is to say, with each new foreground image captured. During the confirmation phase, the following expression must be fulfilled:

$$N(t) \geq N_{MIN} \quad \{t\epsilon[t_D, t_C]\} \tag{2}$$

where N_{MIN} represents the minimum number of candidate regions for smoke to be considered. Below that, changes are associated with a different source and the confirmation phase is interrupted, returning to the pre-detection state.

Another important characteristic of smoke dynamics is their gradual appearance on the scene. Once the first candidate regions are detected, new ones must gradually appear at least until N_{MIN} at $t = t_D$. This can be described by means of two conditions. The first one is:

$$t_D - t_0 \leq T_{D_{MAX}} \tag{3}$$

where $T_{D_{MAX}}$ represents the maximum time interval within which smoke must appear once the first candidate regions are detected. The second condition is:

$$N(t) - N(t - T_F) \leq \Delta_{MAX} \quad \{t\epsilon[t_0, t_C]\} \tag{4}$$

where Δ_{MAX} expresses the maximum permitted growth of candidate regions between two consecutive foreground images during the smoke dynamics. Non-fulfilment of Eq. (3) again cancels the detection and returns the system to the pre-detection state, because the source of the changes (e.g. fog) is considered too slow to behave like smoke. Failing to hold Eq. (4) means that the considered object is growing faster than smoke, and therefore comes from a different source (e.g. a bird flying past).

Finally, smoke does not appear as candidate regions scattered throughout the scene. On the contrary, it is formed by compact clusters. Let us define $Z(t)$ as the number of 8-connected

candidate region clusters. Just like $N(t)$, $Z(t)$ can change with every foreground image. A suitable compactness condition for smoke can be described as:

$$Z(t) \leq Z_{MAX} \quad \{t\epsilon[t_0, t_C]\} \tag{5}$$

where Z_{MAX} is the maximum permitted number of 8-connected candidate region clusters during the smoke dynamics. In other words, failing to hold Eq. (5) means that a different source, for example a flock of birds, is spreading changes in the scene.

As a summary, the flowchart of the algorithm is depicted in Fig. 3. Note that the objective is that the different parameters defined work collaboratively in order to enable successful detection within a set of conditions. Each parameter contributes to dismissing undesired dynamics by encoding a certain characteristic of the spatio-temporal dynamics of a smoke plume. As a whole, they ideally represent a number of features exclusively associated with such dynamics.

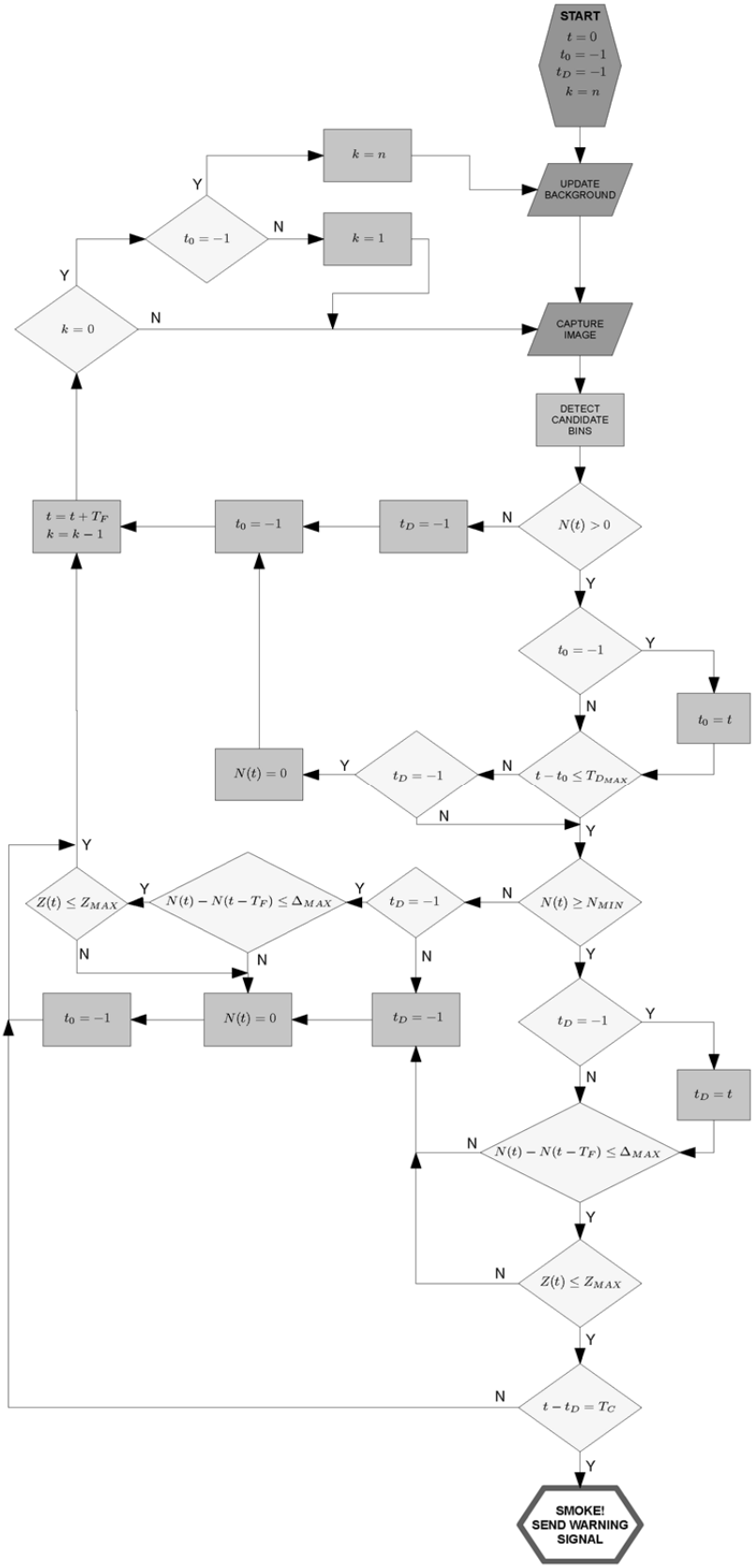

1

2 Fig. 3: Flowchart of the algorithm

Algorithm settings and preliminary tests

In order to set the numerical values of the different parameters of the algorithm and test the algorithm itself, we recorded some sequences in a natural environment, a public park in Seville. Approximately 80 minutes were recorded, with 16 sequences showing the gradual appearance and natural evolution of smoke in scenes in which the background was basically vegetation. Commercial pyrotechnic smoke generators were located at different distances from the three camcorders used, ranging approximately from 20m to 100m. To extract the parameters, 9 of the 16 sequences were analyzed. The rest were used to test the algorithm. Sequences without smoke were also recorded to check the false alarm rate. All this material, in PAL format (720x576px, 25fps), is available at http://www.imse-cnm.csic.es/vmote.

The most important parameter of the algorithm is T_F. Firstly, it must be correlated with the temporal scale of the smoke dynamics, and secondly, the higher its value, the lighter the processing load associated with the algorithm and consequently the lower the power consumption of its implementation. To set T_F, we implemented a very simple motion detector in which the first frame of every sequence analyzed was considered the background. Foreground motion was then determined at pixel level for subsequent frames. Those pixels changing more than a certain threshold would belong to the foreground. By empirically adjusting this threshold in such a way that most of the pixels representing smoke were segmented, we were able to obtain the approximate number of smoke pixels per frame. These are shown in Fig. 4 for the 9 sequences analyzed. This magnitude, highly dependent on the temporal dynamics of smoke, presents a very smooth variation. Indeed, most of the abrupt changes can be tracked by sampling the sequences every second. We thus concluded by setting $T_F = 1\text{s}$. The remaining parameters were adjusted taking into account this value of T_F, so that, from then on, the sequences would be sampled every second.

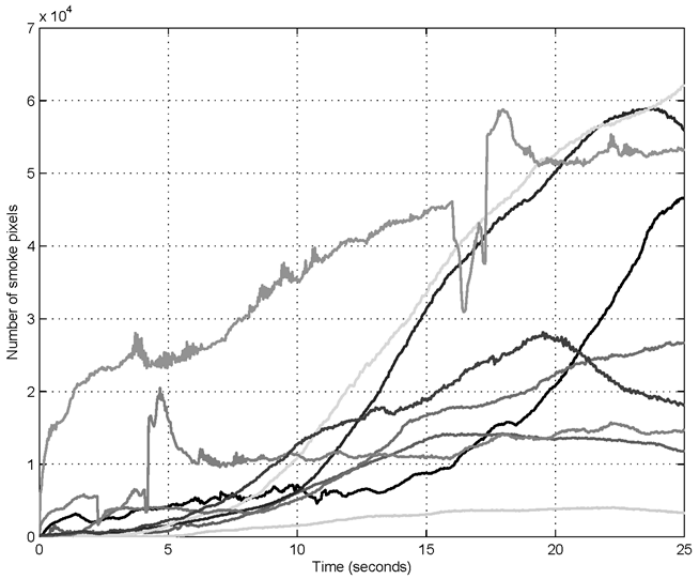

Fig. 4: Number of smoke pixels per frame for each of the 9 different sequences analyzed

Regarding the size of the elementary block of the image plane division, W×H, we computed the average variation in the number of pixels affected when smoke appeared on the scene, and this is shown in Fig. 5. This variation constitutes an estimation of the average size of the regions successively affected by smoke as it spreads across the scene. It can be seen that the minimum value was approximately 200 pixels per second. It should be remembered that the sequences were already being sampled at one frame per second. We therefore decided to set W×H = 15×12px. The dimensions of this elementary block retain the 'width'/'height' ratio of the original full-resolution frame.

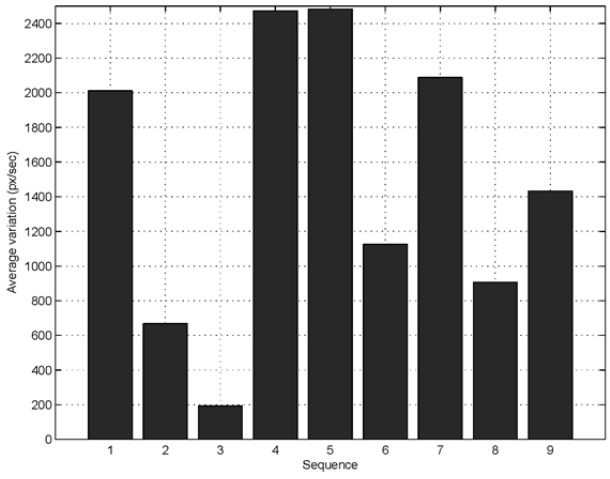

Fig. 5: Average variation in the number of pixels affected by smoke for each sequence.

The next parameter considered is q. In this case, we simply computed the average increase, normalized to the signal range, undergone by the values of the pixels affected by smoke. The result is shown in Fig. 6. Accordingly, we set $q = 10\%$, where the percentage is referred to the signal range. Note that this parameter may require further adjustment in order to accommodate significant seasonal changes in the vegetation making up the background.

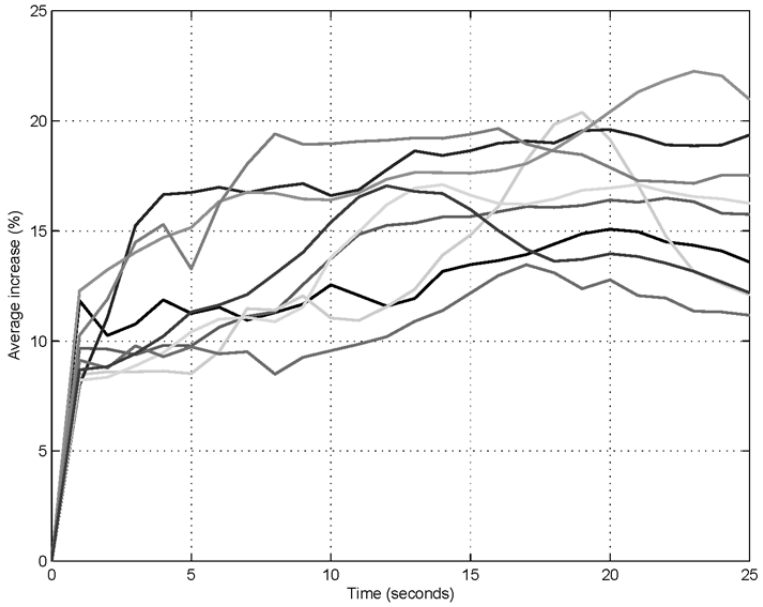

Fig. 6: Normalized average increase in the pixels affected by smoke.

By applying Eq. (1) with the values of W, H and q just set, we were able to obtain the number of candidate regions during the course of each sequence. The minimum value obtained was 17. We set $N_{MIN} = 14$ in order to allow a margin of three candidate regions. This choice implicitly set $T_{D_{MAX}} = 20\text{s}$ and $T_C = 4\text{s}$. At this point, it was easy to adjust the value of Δ_{MAX} by computing the maximum growth rate of the candidate regions for each sequence. The greatest value found was 30 regions per second. We therefore set $\Delta_{MAX} = 30$.

There is one parameter left: Z_{MAX}. To set it, the number of 8-connected candidate region clusters along every sequence was extracted. The maximum value, obtained only once in one of the sequences, was 6. We therefore set $Z_{MAX} = 6$, with no additional margin.

Once the parameters were adjusted (see Table 2), we applied the algorithm to the 7 smoke sequences that were not used for the setting process. Smoke was detected in all of them. The algorithm was also applied to the sequences without smoke. No false alarm was triggered despite the presence of different sources of motion like birds or tree leaves. Therefore, as far as this reduced test bench is concerned, the algorithm achieved a reliability of 100%. As an example, in Fig. 7 we show the dynamics of each and every block making up the image plane division for three sequences up until the time instant at which smoke was detected. Each region is normalized with respect to its value in the background representation. Note that the time instant at which smoke begins to appear in the scene can be easily distinguished due to the progressive increase undergone by the regions affected.

Table 2. Summary of the algorithm settings.

Parameter	Value
T_F	1s
W×H	15×12px
q	10%
N_{MIN}	14
$T_{D_{MAX}}$	20s
T_C	4s
Δ_{MAX}	30
Z_{MAX}	6

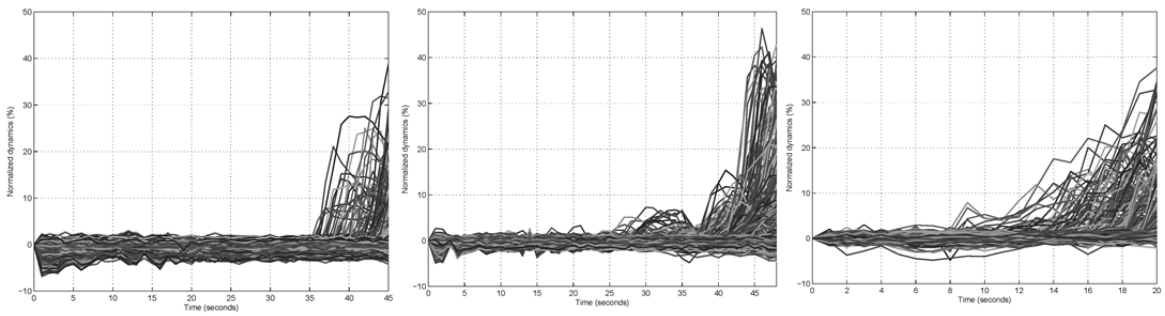

Fig. 7: Normalized dynamics (%) of all the regions making up the image plane division for three recordings until smoke was detected.

Field tests with a commercial system

The next step in our incremental approach to the problem, once the vision algorithm had been tuned for smoke detection, was to programme it into a commercial autonomous vision system. The objective was to carry out on-site surveillance while checking the algorithm in other scenarios and dealing with potential operational problems. The system chosen was *EyeRIS*^{TM} v1.2, a general-purpose autonomous vision system built by AnaFocus Ltd. (http://www.anafocus.com). The reasons for this choice were a) the availability of this system in the laboratory when we had finished the preliminary tests on the algorithm and b) the application development kit with which it is supplied and which enables the fast implementation of standalone applications. The only modification to the algorithm for its implementation in *EyeRIS*^{TM} was the image plane division. This modification is mandatory in order to keep the other parameters unaltered. The elementary block was adjusted to the system's QCIF resolution of 176×144px. Accurate adjustment would require elementary blocks of 3.66×3px, resulting from applying the reduction of resolution to the original size of these blocks, 15×12px. We finally decided to set blocks of 4×4px for a slight increase in image simplification.

The algorithm was first tested in the laboratory. To this end, some of the video recordings containing smoke sequences were displayed on a computer screen on which *EyeRIS*^{TM} was focused. We also made sure that the algorithm's behaviour could be supervised in real time from a PC connected to the vision system. This real-time supervision resulted very useful in detecting minor problems during the field test carried out in the "Las Navas - El Berrocal" public forest in the province of Seville (37.85N, 6.04W). Two controlled burns of forest debris like those in Fig. 8 were overseen by personnel from the Andalusian Forest Fire Suppression and Prevention Service (INFOCA). The *EyeRIS*^{TM} system was placed on top of a three-meter high pole powered by a commercial 9V battery connected to a DC-to-DC converter which supplied it with the adequate voltage. A camcorder was also placed on top of the pole in order to

record the sequences from the same position as *EyeRIS*^{TM}. The arrangement of both the *EyeRIS*^{TM} system and the camcorder can be seen in Fig. 9. The pole was placed at a distance of around 50 meters from the forest debris. Another camcorder was placed on a tripod at different positions around the burns to record them from different perspectives. All the sequences can be found and downloaded at http://www.imse-cnm.csic.es/vmote.

Fig. 8: Forest debris burnt during the field tests.

Fig. 9: Arrangement of the EyeRIS^{TM} system (on the left in both photos) and the commercial camcorder (on the right in both photos) during the field tests.

Smoke was detected without false alarms in both burns. In the first, the alarm was triggered at 2min 50sec from ignition whereas in the second the alarm was delivered after 57sec. Some consecutive frames captured by *EyeRIS*^{TM} during the first burn along with their corresponding candidate regions are shown in Fig. 10. The evolution of $N(t)$ and $Z(t)$ is depicted in Fig. 11 for both burns. The most remarkable aspect about the results is the algorithm's ability to filter motion other than smoke. In fact, it can be seen from the image sequences extracted that two potential sources of false alarms like the movement of tree leaves due to wind and the movement of people crossing the scene are mostly filtered. The alarms are therefore undoubtedly triggered by the smoke arising from the burns.

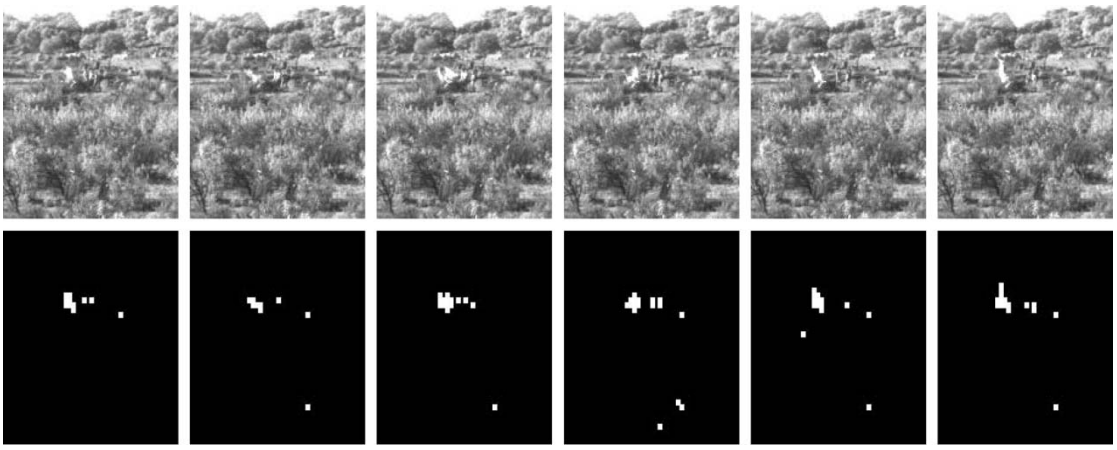

Fig. 10: Consecutive frames captured by *EyeRIS*^{TM} (first row) and their corresponding candidate bins (second row) during the first controlled burn.

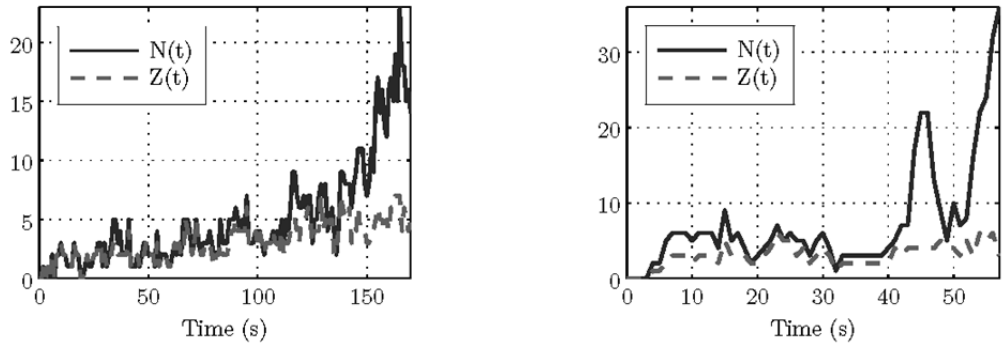

Fig. 11: Evolution of $N(t)$ and $Z(t)$ for the first and second burn respectively.

Implementation of a vision-enabled WSN node

Once the suitability of the algorithm for the early, on-site detection of forest fires was confirmed, we finally addressed the implementation of a prototype vision-enabled WSN node. A fundamental element of this node is the smart imager (Fernández-Berni *et al.* 2011-1). This chip, called *FLIP-Q*, carries out image sensing, focal-plane processing running concurrently with the sensing, and analog-to-digital conversion at very low energy cost – 5.6mW in the worst case. In this way, our imager can output from full-resolution digital images to different simplified representations of the scene which can then be reprogrammed in real time according to the results of the image processing. One of these simplified representations is the division of the image plane into regions of W×H pixels and the subsequent computation of their mean value, an operation required by the smoke detection algorithm. It is achieved in parallel for all the regions, no matter their size, the only energy cost being the power needed to capture a frame. This efficiency is crucial if the nodes are to have a long lifetime.

Wi-FLIP (Fernández-Berni *et al.* 2011-2) is the vision-enabled WSN node resulting from the integration of *FLIP-Q* and *Imote2*, a commercial WSN platform from MEMSIC Corp. (www.memsic.com). This platform is built around a microprocessor which can operate in a low voltage low-frequency mode, hence allowing very low power operation. An 802.15.4-compliant radio is also integrated into the *Imote2* system. Two snapshots of *Wi-FLIP* are shown in Fig. 12.

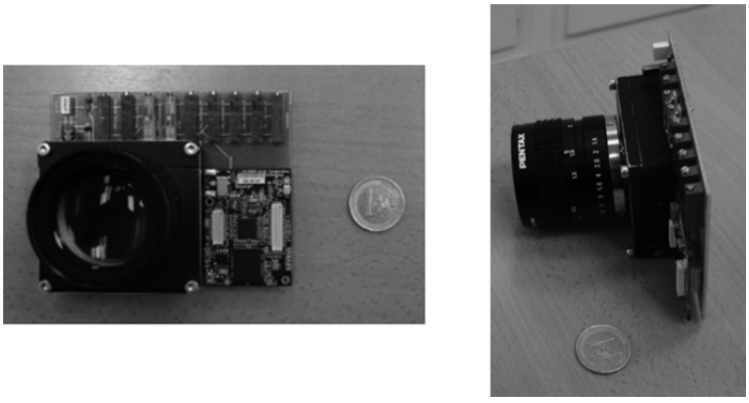

Fig. 12: *Wi-FLIP*, a 10cm×8cm vision-enabled node for wireless applications.

Results and Discussion

The smoke detection algorithm was programmed into *Wi-FLIP*. No additional modification was necessary as the resolution of *Wi-FLIP* is the same as *EyeRIS*^{TM}. Furthermore, since the programming languages used in both systems are similar, the adaptation of the code written for *EyeRIS*^{TM} to *Wi-FLIP* was quite simple. To attain the prescribed frame rate for the algorithm, 1fps, the microprocessor had to be set to 416MHz. This represented a power consumption of around 155mA; that is, a node lifetime of around 10 hours for the three AAA batteries powering the system. A small solar panel could be also used for continuous operation, but this option has not yet been tested. Thanks to the availability of radio communication in *Wi-FLIP*, full-resolution images are constantly sent via radio to a remote base station connected to a PC every 15s after an alarm is triggered. This base station can be located within a range of 30m. In a real deployment, the information transmitted by *Wi-FLIP* would be relayed by successive nodes until it reached the corresponding base station.

As a first step, we arranged new tests in the same public park where the video sequences for the algorithm settings were recorded. Commercial pyrotechnics were again used as smoke generators The setting up of these tests was complicated by strong gusts of wind. Nevertheless, no false alarm was triggered during eight sequences of smoke generation and detection was successful in five of them. Smoke was not successfully detected in the others because, due to the wind, the pyrotechnic material burnt out before it had entered the field of view of *Wi-FLIP* sufficiently to be registered. In a real fire, smoke spreads steadily and should therefore eventually be detected. Some frames captured by a commercial camcorder and the corresponding smoke segmentation realized by *Wi-FLIP* are shown in Fig. 13. The last image corresponds to the first alarm image sent via radio.

Fig. 13: Smoke segmentation and alarm image from *Wi-FLIP*.

The latest test consisted of the prescribed burning of a 95m×20m area of vegetation in the "Las Navas - El Berrocal" public forest, once again in collaboration with the Andalusian Forest Fire Supression and Prevention Service. This area featured a smooth slope and different species of shrubs: *Genista hirsuta*, *Lavandula stoechas* and *Cistus ladanifer*. According to the Rothermel fire-spread model (Rothermel 1972) these constitute fuel model 6. *Wi-FLIP* was placed about 80m away from the aforementioned area and monitored all the activity occurring in it for over two hours. A commercial camcorder also recorded a number of sequences. Two snapshots taken during the test are shown in Fig. 14. More material can be found at http://www.imse-cnm.csic.es/vmote. With regard to the results obtained, it should first be mentioned that, prior to the burn, the area was mechanically divided into three zones of similar sizes according to the density of the vegetation. The first zone presented very sparse vegetation. This meant that very thin smoke was generated, and produced the only case in which *Wi-FLIP* did not trigger an alarm. In the second zone, the vegetation was denser and the smoke which appeared was therefore thicker. A first alarm was therefore triggered 5m 28sec after ignition. With the fire still active, we reset *Wi-FLIP* so that the algorithm started to run again from zero. A new alarm was triggered 2m 40sec after this reset operation. Finally, the third zone featured the densest vegetation. A first alarm was delivered 3m 29sec after the fire was started there. We then repeated the *Wi-FLIP* reset operation performed for the second zone, and a second alarm was triggered 1m 9sec afterwards. These alarms triggered even with the fire already spreading demonstrate the algorithm's capability to detect the presence of fire in a scene, regardless of its

characteristics at any given moment. The first image sent via radio by Wi-FLIP for one of the four alarms triggered is shown in Fig. 15. It is also especially remarkable that, despite the fact that a great deal of people and vehicles were moving around, no false alarm was triggered either before or after the prescribed burn. This is a key point concerning the reliability of our vision-enabled WSN node.

Fig. 14: Snapshot taken during the latest test carried out.

Fig. 15: Image sent via radio by *Wi-FLIP* for one of the alarms triggered.

These results are promising, but we still think that several aspects of our prototype node must be improved. The current lifetime of the system is competitive, taking into account that it can be powered by small commercial batteries for around 10 hours. However, the objective is to have the nodes running autonomously for at least several weeks. Energy harvesting is therefore absolutely mandatory, even if the power consumption of the system is significantly reduced. We have also noticed that the parameters of the algorithm still require further tuning. Specifically, earlier detection could be probably attained with a longer time interval $T_{D_{MAX}}$. Its current value forced the algorithm to dismiss spatio-temporal dynamics which corresponded to the beginning of the fire, thus delaying the alarm trigger. The performance of *Wi-FLIP* has not yet been analyzed in a real deployment. In such conditions, each node must deal with different kinds of information coming from the network – the updating of routing tables, radio beacons, alarms etc. – while keeping the algorithm working correctly. This is not a trivial issue and must be adequately addressed. Finally, we estimate that at least four sensors per km^2 will be necessary for adequate coverage, although this figure will heavily depend on the characteristics of the area to be surveyed. Nevertheless, it is important to reemphasize that vision-enabled wireless sensor networks are intended to enable low-cost fine-grained surveillance of locations with a high fire danger index. They are not, in principle, intended to cover very extensive areas with lots of sensors. Cost estimates for a system with the proposed areal coverage are really difficult to provide for the time being and depend on many parameters which would have to be taken into careful consideration before the system could be marketed: smart imager integration technology, the number of samples manufactured, the microprocessor chosen to run the system, the transceiver used etc. In any case, the scalable nature of the proposed system enables progressive implementation without incurring the huge costs of current automatic ground systems.

Conclusions

The incorporation of vision into wireless sensor network nodes represents a remarkable step forward in the possibilities of these networks in terms of forest fire detection. In this paper, a new framework is defined by merging ground detection systems and WSN-based monitoring systems in order to achieve early detection with greater robustness and reliability. It is based on the design of a reliable vision algorithm and the ad-hoc implementation of a low-power smart imager. These two key elements have been integrated into a prototype vision-enabled WSN node. The results of the field tests carried out have demonstrated that the proposed approach constitutes a sound basis for the future development of fine-grained spatio-temporal sensing grids. Such future development should take into account numerous aspects not yet studied, for example how the performance of the vision algorithm varies for sensor-plume distances outside the range considered. Specifically, assuming that at least four sensors per km^2 will be necessary for adequate coverage, future tests should check the whole detection process for greater distances than those of the experiments performed in this paper. Other features to be also explored are energy harvesting techniques, further tuning of the parameters or fine adjustment of the number of sensors for adequate coverage.

Acknowledgements

The authors would like to express their deep gratitude to Mr. Manuel Larios de la Carrera (deputy director) and Mr. Salvador Benítez Moscoso (director), from the INFOCA Operational Center for the province of Seville, for arranging the burns. This work is funded by MICINN (Spain) through project TEC2009-11812, co-funded by the European Regional Development Fund, by the Office of Naval Research (USA), through grant N000141110312, by the Spanish Ministry of Science and Innovation through Project IPT-2011-1625-430000 and by the Spanish Centre for Industrial Technological Development, co-funded by the European Regional Development Fund, through Project IPC-20111009.

References

Akyildiz IF, Su W, Sankarasubramaniam Y, Cayirci E (2002) A survey on sensor networks. *IEEE Communications Magazine* **40**(8), 102–114.

Akyildiz IF, Melodia T, Chowdhury KR (2007) A survey on wireless multimedia sensor networks. *Computer Networks* **51**(4), 921-960.

Arrue BC, Ollero A, Martínez de Dios JR (2000) An intelligent system for false alarm reduction in infrared forest fire detection. *IEEE Intelligent Systems*, **15**(3), 64-73.

Chaczko Z, Ahmad F (2005) Wireless sensor network based system for fire endangered areas. In 'Third Int. Conf. on Information Technology and Applications', Sidney, Australia, 477–484.

Chen T, Yin Y, Huang S, Ye Y (2006) Smoke detection for early fire-alarming system based on video processing. In 'IEEE Int. Conf. on Intelligent Information Hiding and Multimedia Signal Processing', Pasadena (CA), USA, 427-430.

de Vries JS, Kemp RA (1994) Results with a multispectral autonomous wildfire detection system. In 'Proc. SPIE, Infrared Technology XX', San Diego (CA), USA, 18-28.

den Breejen E, Breuers M, Cremer F, Kemp RA, Roos M, Schutte K, de Vries JS (1998) Autonomous Forest Fire Detection. In 'III International Conference on Forest Fire Research', Coimbra, Portugal.

Doolin D, Sitar N (2005) Wireless sensors for wildfire monitoring. In 'SPIE Symposium on Smart Structures and Materials', San Diego, USA, 477–484.

Eren G, Akan OB (2005) Multimedia communication in wireless sensor networks. *Annales des Telecommunications* **60**(7-8), 872-900.

Fernández-Berni J, Carmona-Galán R, Carranza-González L (2008) A vision-based monitoring system for very early automatic detection of forest fires. In 'First Int. Conf. on Modelling, Monitoring and Management of Forest Fires', Toledo (Spain), 161-170.

Fernández-Berni J, Carmona-Galán R, Carranza-González L (2009) A VLSI-oriented and power-efficient approach for dynamic texture recognition applied to smoke detection. In 'Int. Conf. on Computer Vision Theory and Applications', Lisbon (Portugal), 307-314.

Fernández-Berni J, Carmona-Galán R, Carranza-González L, Cano-Rojas A, Martínez-Carmona JF, Rodríguez-Vázquez A, Morillas-Castillo S (2010) On-site forest fire smoke detection by low-power autonomous vision sensor. In 'VI International Conference on Forest Fire Research', Coimbra, Portugal.

Fernández-Berni J, Carmona-Galán R, Carranza-González L (2011-1). A QCIF resolution focal-plane array for low-power image processing. *IEEE Journal of Solid-State Circuits* **46**(3), 669-680.

Fernández-Berni J, Carmona-Galán R, Liñán-Cembrano G, Zarándy A, Rodríguez-Vázquez A (2011-2) Wi-FLIP: A wireless smart camera based on a focal-plane low-power image processor. In 'Fifth ACM/IEEE Int. Conf. on Distributed Smart Cameras', Ghent (Belgium).

Fierens PI (2009) Number of sensors versus time to detection in wildfires. *International Journal of Wildland Fire* **18**, 825–829.

Fire Watch (2004). Fire Watch: a commercial forest fire detection system. http://www.fire-watch.de.

Gómez-Rodríguez F, Pascual-Peña S, Arrue BC, Ollero A (2002) Smoke detection using image processing. In 'IV International Conference on Forest Fire Research', Coimbra, Portugal.

Hefeeda M (2007) Forest fire modelling and early detection using wireless sensor networks. Technical report, School of Computing Science, Simon Fraser University.

INSA (2000) FUEGO instrument design, prototype, construction and validation. Technical report, INSA Ingeniería y Servicios Aeroespaciales.

Jacquemoud S, Verdebout J, Schmuck G, Andreoli G, Hosgood B, Hornig SE (1994) Investigation of Leaf Biochemistry by Statistics. In 'Geoscience and Remote Sensing Symposium', vol. 2 1239-1241.

Kremens R, Faulring J, Gallagher A, Seema A, Vodacek A (2003) Autonomous field-deployable wildland fire sensors. *International Journal of Wildland Fire* **12**, 237–244.

Krstinic D, Stipanicev D, Jakovcevic T (2009) Histogram-based smoke segmentation in forest fire detection system. *Information Technology and Control* **38**(3) 237-244.

Kuhrt E, Knollenberg J, Mertens V (2001) An automatic early warning system for forest fires. *Annals of Burns and Fire Disasters* **XIV**(3), 151-155.

Machado R, Ribeiro G, Ditmore A, Romano M, Meireles W (2010) Online Paradise: A wireless sensor network applied in the prevention and detection of forest fires. In 'VI International Conference on Forest Fire Research', Coimbra, Portugal.

Pottie, G., Kaiser, W. (2000) Wireless integrated network sensors. *Communication of the ACM* **43**(5), 51–58.

Rothermel RC (1972) A mathematical model for predicting fire spread in wildland fuels. Research paper, Intermountain Forest and Range Experiment Station, USDA Forest Fire Service.

Schroeder D (2004) Evaluation of three wildfire smoke detection systems. Advantage Report, FERIC Forest Engineering Research Institute of Canada, **5**(24).

Schroeder D (2005) Operational Trial of the ForestWatch Wild_re Smoke Detection System. Advantage Report, FERIC Forest Engineering Research Institute of Canada, **6**(17).

1 Sistema Bosque (1999) Sistema Bosque, Andalusian Forest Fire Suppression and Prevention
2 Service. http://waste.ideal.es/sistemabosque.htm.

3 Son B, Her Y, Kim J (2006) A design and implementation of forest-fires surveillance system
4 based on wireless sensor networks for South Korea mountains. *International Journal of*
5 *Computer Science and Network Security* **6**(9), 124–130.

6 Stipanicev D, Stula M, Krstinic D, Seric L, Jakovcevic T, Bugaric M (2010) Advanced
7 automatic wildfire surveillance and monitoring network. In 'VI International Conference on
8 Forest Fire Research', Coimbra, Portugal.

9 Toreyin U, Dedeoglu Y, Enis-Cetin A (2007) Computer vision-based forest fire detection and
10 monitoring system. In 'International Wildland Fire Conference', Seville, Spain

11 Vicente J, Guillemant P (2002) An image processing technique for automatically detecting
12 forest fires. *International Journal of Thermal Sciences* **41**(12), 1113-1120.